第 43 卷 第 21 期/2023 年 11 月/光学学报 研究论文

光学学报

基于功能化水凝胶的肿瘤源性外泌体高灵敏检测

杨朝雁[1,2]，赵书瑾[1]，王子烨[1]，刘娇[1]，宗慎飞[2]，王著元[2**]，李炳祥[1*]，崔一平[2]

[1]南京邮电大学电子与光学工程学院，柔性电子（未来技术）学院，江苏 南京 210023；

[2]东南大学电子科学与工程学院，江苏 南京 210096

摘要 提出一种外泌体检测新方法，通过将表面增强拉曼散射（SERS）纳米探针固定在核酸适体（DNA）功能化水凝胶中，实现对肿瘤源性外泌体的高灵敏度光学检测。SERS纳米探针被用于识别肿瘤源性外泌体并产生指纹光学信号。SERS活性DNA功能化水凝胶（简称“SD水凝胶”）作为传感器，不仅提供了用于生物识别的三维反应位点，而且可放大SERS纳米探针的光学信号。选择性地与靶外泌体结合后，SERS纳米探针脱离SD水凝胶，导致SERS信号减弱，从而实现光学检测。通过SERS信号变化，SD水凝胶可以定量、灵敏地检测肿瘤源性外泌体，浓度检测限（LOD）约为22 μL^{-1}。该SD水凝胶将为临床癌症诊断提供一种新的技术手段。

关键词 生物光学；表面增强拉曼散射光谱技术；光学检测；外泌体；纳米探针；水凝胶

中图分类号 O433 **文献标志码** A **DOI**：10.3788/AOS230823

1 引 言

外泌体是一种细胞外囊泡，尺寸范围为30～150 nm[1]，存在于多种体液中，包括血液、泪液、尿液和母乳[2]。通常，外泌体具有磷脂双层膜结构，其膜表面为特定蛋白质，膜内部是生物大分子，例如碳水化合物、蛋白质和核酸[3-4]。在细胞内的物质交换和通讯中，外泌体起着至关重要的作用[5-6]。除此之外，与正常细胞相比，肿瘤细胞分泌更多具有肿瘤特异性蛋白的外泌体[7-9]，这使得肿瘤源性外泌体成为一种重要的癌症生物标志物[10-11]。因此，肿瘤源性外泌体检测可以为癌症临床诊断提供关键信息。目前，已经建立多种外泌体检测方法，如蛋白质印迹法、聚合酶链式反应法（PCR）和酶联免疫吸附法（ELISA）[12-13]。然而，这些方法仍然存在不足，如操作繁琐、准确性有限等。因此，亟需开发一种操作方便、灵敏度高的外泌体检测方法。

表面增强拉曼散射（SERS）光谱以其独特的性质在生物检测领域得到了广泛应用[14-15]。基于SERS的检测方法可以达到单分子检测水平[16-17]。此外，鉴于对光漂白的高抗性，基于SERS的定量检测可以提供更可靠的结果[18-19]。更重要的是，由于指纹特性和窄光谱带宽，SERS可以提供出色的多路检测能力[20-22]。近年来，基于SERS的外泌体检测方法蓬勃发展[23-26]。许多材料已经与SERS探针结合，以获得最佳的检测结果。例如：Wang等[27]利用磁珠联合SERS光谱收集并检测目标外泌体；Pan等[28]使用MoS_2纳米片增强拉曼信号，提高外泌体检测灵敏度。为提高生物相容性和灵敏度，仍需进一步开发外泌体检测方法。

水凝胶是一种由亲水性聚合物交联而成的水溶胀性聚合物材料，具有三维（3D）网络结构和良好的生物相容性[29]。水凝胶的多孔结构特征与细胞外基质类似[30]，生物分子在水凝胶中可以保持其固有的结构和功能特征。在水凝胶形成过程中，经丙烯酸酯改性的DNA能够容易地与水凝胶结合，以识别和固定生物分子[31]。同时，水凝胶的3D结构可以提供更多反应位点。因此，水凝胶被广泛应用于生物检测。

本文通过将生物相容性3D水凝胶与SERS纳米探针相结合，构建了一种光学检测平台，讨论了该平台的结构和光学性质，并研究了其生物检测能力。此外，提出一种高效、灵敏的肿瘤源性外泌体检测方法，以期为癌症早期诊断提供新的技术途径。

2 实验部分

2.1 检测原理

SERS活性DNA功能化水凝胶（以下简称“SD水凝胶”）检测原理如图1所示。SD水凝胶由两部分组成，分别是用于识别外泌体和产生SERS信号的SERS

收稿日期：2023-04-17；**修回日期**：2023-05-17；**录用日期**：2023-06-12；**网络首发日期**：2023-09-20

基金项目：国家重点研发计划（2022YFA1405000）、国家自然科学基金（RK106LH21001，62175030，62175027）、江苏省自然科学基金重大项目（BK20212004）、南京邮电大学人才招聘自然科学研究启动基金（NY222105，NY222122，NY222080，NY222121）

通信作者：*bxli@njupt.edu.cn；**wangzy@seu.edu.cn

纳米探针[图 1(a)],以及用于固定SERS纳米探针和增强拉曼信号的DNA功能化聚丙烯酰胺水凝胶(以下简称“DPAAm水凝胶”)。这两个部分通过DPAAm水凝胶中的丙烯酸酯DNA连接[图 1(b)]。图 1(c)展示了SD水凝胶对肿瘤源性外泌体的检测原理。这种SD水凝胶利用SERS纳米探针来区分肿瘤和正常细胞来源外泌体之间的表面特异性蛋白差异。具体原理是:肿瘤源性外泌体的出现导致SERS纳米探针与丙烯酸酯DNA之间的相互作用被破坏,引起SERS纳米探针脱离水凝胶,最终减弱水凝胶中的SERS信号。

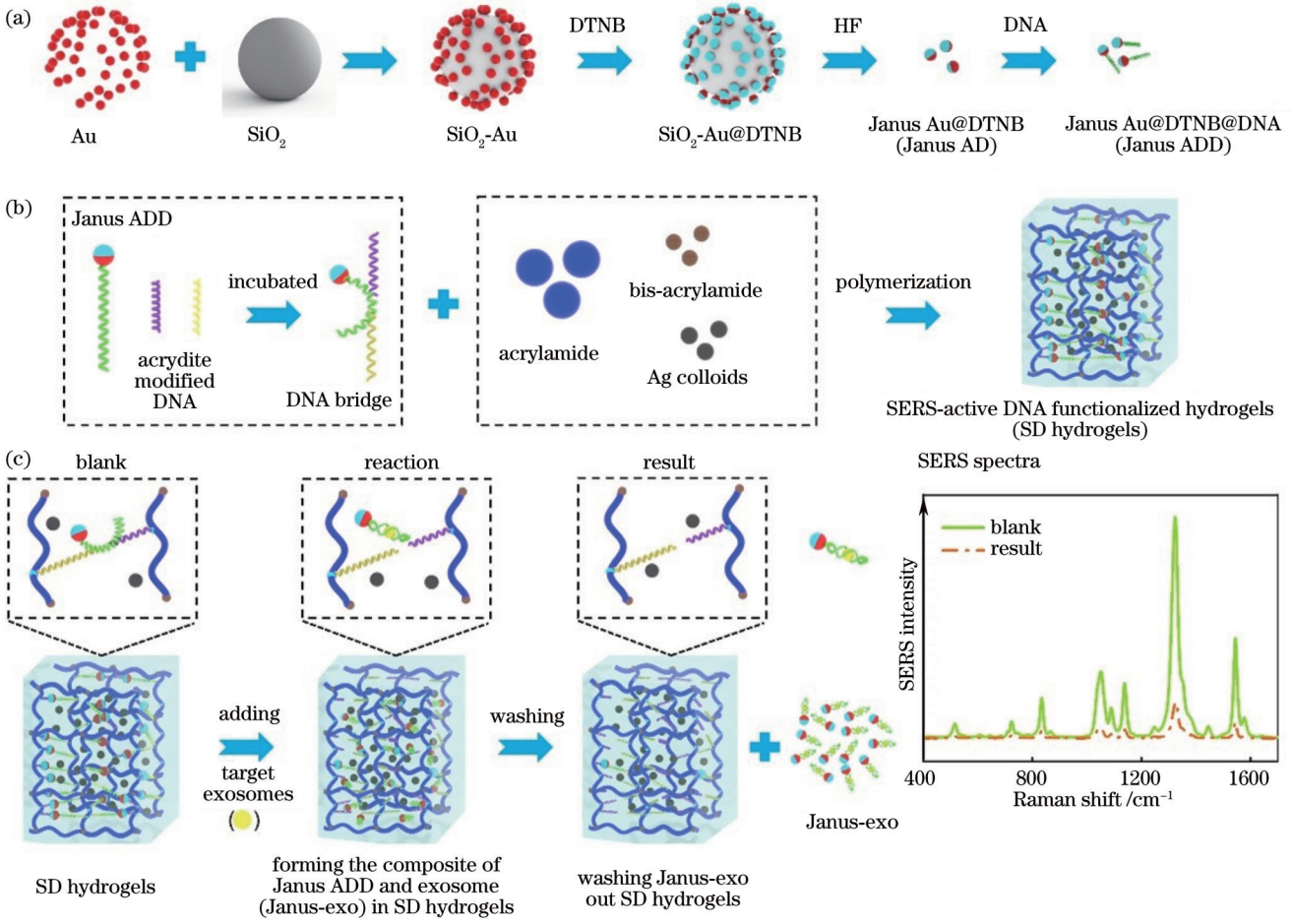

图 1　基于SD水凝胶的外泌体检测方法说明(图像不按比例缩放)。(a)SERS纳米探针的制备;(b)SD水凝胶的制备;(c)基于SD水凝胶的肿瘤源性外泌体检测原理

Fig. 1　Illustration of SD hydrogel-based exosome detection method (images are not to scale). (a) Preparation of SERS nanoprobes; (b) preparation of SD hydrogels; (c) principles of SD hydrogels for detection of tumor-derived exosomes

2.2　实验材料

氯金酸三水合物($HAuCl_4·3H_2O$)、原硅酸四乙酯(TEOS)、(3-氨基丙基)三甲氧基硅烷(APTMS)和硝酸银($AgNO_3$)购自 Alfa-Aesar;丙烯酰胺、双丙烯酰胺、过硫酸铵(APS)、四甲基乙二胺(TEMED)、硼氢化钠($NaBH_4$)、二水合双(对-磺酰苯基)苯基膦化二钾盐(BSPP)和5,5′-二硫代双(2-硝基苯甲酸)(DTNB)购自 Sigma-Aldrich;氢氟酸(HF)和氢氧化铵($NH_3·H_2O$)购自上海凌峰化学试剂有限公司;无水乙醇和二水合柠檬酸钠($C_6H_5Na_3O_7·2H_2O$)购自国药集团化学试剂有限责任公司;磷酸缓冲盐(PBS,pH=7.4)购自南京布克曼生物科技有限公司。所有寡核苷酸均由生工生物科技(上海)有限责任公司合成(表 1),膜标志染料(DID)由凯基生物技术有限公司生产。所有实验中均使用电阻率为 18.2 MΩ·cm 的去离子水(Millipore Milli-Q级)。

2.3　实验过程

2.3.1　SD水凝胶合源成

通过使用先前报道[32]的方法合成BSPP封端的金纳米粒子(Au NPs):首先,将 20 μL $HAuCl_4·3H_2O$(质量分数为 10%)和 1.47 mg $C_6H_5Na_3O_7·2H_2O$ 放入 20 mL 去离子水中;然后,将上述溶液与 600 μL $NaBH_4$(0.1 mol/L)搅拌混合,并将反应溶液在室温下储存 24 h,以水解过量的 $NaBH_4$;最后,向溶液中加入 3 mg BSPP,并在室温下振荡,放置过夜,获得 BSPP 封端 Au NPs。

根据文献[33]的报道,制备 APTMS 功能化的二氧化硅纳米粒子(SiO_2 NPs),并将 20 mL BSPP 封端

表 1 适体序列信息

Table 1 Summary of aptamers

Aptamer	Sequence (5′ to 3′)
P1	5′-acrydite-AAACAG TAC TCA GGT-$(CH_2)_6$-NH_2-3′
P2	5′-acrydite-AAAGGT GGG GTG GGA-$(CH_2)_6$-NH_2-3′
CD63-HER2 (CH)	5′-SH-$(CH_2)_6$-GGG CCG TCG AAC ACG AGC ATG GTG CGT GGA CCT AGG ATG ACC TGA GTA CTG TCC CAC CCC ACC TCG CTC CCG TGA CAC TAA TGC TA-3′
CD63-HER2 complementary (CHC)	5′-TA GCA TTA GTG TCA CGG GAG CGA GGT GGG GTG GGA CAG TAC TCA GGT CAT CCT AGG TCC ACG CAC CAT GCT CGT GTT CGA CGG CCC-3′

Au NPs溶液与6 mL APTMS功能化SiO_2 NPs混合搅拌4 h。随后，加入25 μL DTNB(10 mmol/L)搅拌6 h。以7000 r/min的转速离心两次(每次20 min)后，将沉淀物重悬于1 mL去离子水。使用960 μL HF(质量分数为4%)溶液去除SiO_2 NPs后，获得表面被DTNB部分修饰的Au NPs(记作Janus AD)溶液。将溶液离心至pH接近中性后，将10 μL DNA(100 μmol/L)与1 mL Janus AD溶液混合反应，获得拉曼信号分子DTNB与DNA共同修饰的Janus ADD。离心去除溶液中未结合的DNA。为制备Janus ADCH，仅需将DNA替换为CD63-HER2(CH)适体。

为制备SD水凝胶，首先将丙烯酸酯改性的DNA1(P1)和DNA2(P2)与Janus ADD孵育过夜以形成DNA桥结构。Ag胶体根据先前报道[34]的方法制备。然后，将DNA桥、40%凝胶溶液(丙烯酰胺∶双丙烯酰胺在Ag胶体中的质量比为39∶1)和TBE缓冲液以1∶1∶2的体积比混合。该混合物的最终凝胶百分比为10%。为引发聚合，将50 mg APS溶解在500 μL水中，再加入25 μL TEMED，制备新鲜引发剂溶液。随后，将引发剂与凝胶混合物以7∶200的体积比混合。最后，用TBE缓冲液终止凝胶聚合反应。将获得的SD水凝胶在TBE缓冲液中浸泡3次，以去除游离单体、引发剂和未结合的DNA桥(每次浸泡至少3 h)。为制备SCH水凝胶，仅需将Janus ADD替换为Janus ADCH。

2.3.2 SKBR3外泌体检测

1)细胞培养

SKBR3细胞购自中国科学院典型培养物保藏委员会细胞库，在标准细胞培养条件下增殖(5% CO_2，37 ℃)。SKBR3细胞在补充有10%胎牛血清(GIBCO)和1%青霉素-链霉素(南京凯基生物技术有限公司)的DMEM培养基中培养。

2)外泌体收集

将细胞接种到细胞培养瓶(Corning，25 cm^2)中并培养至70%汇合。将含有外泌体的培养基收集在无菌离心管。通过超速离心法从培养基中分离外泌体[11]。使用纳米颗粒跟踪分析仪(NTA；Malvern，NanoSight NS300)测量外泌体的浓度，其值为2.20×10^7 μL^{-1}。

3)外泌体检测

首先，将不同浓度SKBR3外泌体与SCH水凝胶在4 ℃下孵育24 h。然后，将SCH水凝胶在PBS缓冲液中浸泡3次(每次浸泡至少3 h)。最后，将SCH水凝胶在烘箱中干燥以进行光谱收集。

2.4 仪器

使用超速离心机(Optima XPN-100，Beckman Coulter)进行超速离心反应。通过透射电子显微镜(TEM；FEI-Tecnai G2T20)采集TEM图像。使用扫描电子显微镜(SEM；FEI Inspect F50)获得SEM图像。通过Malvern Zetasizer(Nano ZS 90)进行Zeta电位测量。通过UV-Vis吸收分光光度计(UV3600，岛津)采集消光光谱。通过共聚焦显微镜(FV1000，Olympus)在10×物镜下获得荧光图像。使用Horiba T64000在10×物镜和632.8 nm激光照射下采集SERS光谱。通过配备有405 nm(50 mW)、488 nm(100 mW)、561 nm(100 mW)和642 nm(150 mW)激光器的蔡司Elyra P.1显微镜获得外泌体的超分辨率图像，并使用Andor EM-CCD相机(iXon DU897)在100×/1.46油浸物镜下记录结果。使用蔡司Zen 2012软件分析超分辨成像数据。所有的光学测量结果都在室温下获得。

3 结果与讨论

3.1 SERS探针的表征

SERS探针的成功制备是检测肿瘤源性外泌体的先决条件。为获得SERS探针，首先制备Au NPs和APTMS修饰的SiO_2 NPs[32-33]。图2(a)显示Au NPs和SiO_2 NPs具有相反的Zeta电位。然后，利用Au NPs与SiO_2 NPs之间的静电相互作用制备SiO_2-Au NPs。图2(b)展示了SiO_2-Au NPs的TEM图像。结果清楚地表明，Au NPs分布在SiO_2 NPs表面。通过Au-S键的形成将DTNB分子连接到SiO_2-Au NPs上。DTNB具有两个功能：第一，它取代了Au NPs表面的BSPP稳定剂；第二，它提供了一个可区分的拉曼信号。所获得的DTNB改性SiO_2-Au NPs (SiO_2-

Au@DTNB)显示了－24 mV的Zeta电位[图2(a)]。通过HF蚀刻SiO_2 NPs,获得了表面部分修饰DTNB的Janus Au@DTNB(记作Janus AD)。Janus AD的TEM图像如图2(c)所示,其在形态上与初始Au NPs一致。Janus AD的Zeta电位仍然为负性。最后,DNA适体与Janus AD反应形成Janus Au@DTNB@DNA(记作Janus ADD)。由于Au与巯基之间的相互作用力较强,Janus AD表面上的BSPP稳定剂被巯基修饰的DNA适体取代。与Janus AD相比,Janus ADD的Zeta电位从－15.3 mV降至－28.9 mV[图2(a)]。这一现象表明,DNA适体已经成功修饰至Janus AD表面。

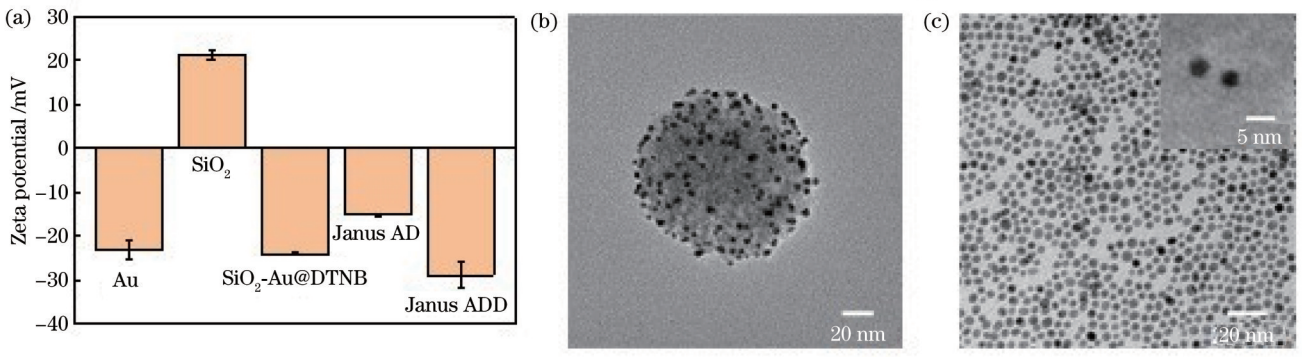

图2　SERS探针的特性。(a)通过动态光散射(DLS)测量Au、SiO_2、SiO_2-Au@DTNB、Janus AD和Janus ADD的Zeta电位;(b)SiO_2-Au和(c)Janus AD的TEM图像

Fig. 2　Characteristics of SERS probes. (a) Zeta potential of Au, SiO_2, SiO_2-Au@DTNB, Janus AD, and Janus ADD measured by dynamic light scattering (DLS); TEM images of (b) SiO_2-Au and (c) Janus AD

图3(a)显示了Au、SiO_2-Au@DTNB、Janus AD和Janus ADD的消光光谱。Au NPs在大约520 nm处显示出典型的吸收峰,这个峰位在SiO_2-Au@DTNB、Janus AD和Janus ADD中红移至522 nm,并且半峰全宽(FWHM)变大。峰位的红移可以归因于DTNB的添加。图3(b)展示了SiO_2-Au@DTNB、Janus AD和Janus ADD的SERS光谱。显然,Janus ADD具有独特的拉曼信号,主频带位于1333 cm^{-1},这与SiO_2-Au@DTNB和Janus AD一致。此外,DNA的修饰可能引起Janus AD纳米粒子轻微聚集,进而导致Janus ADD的SERS信号增强。以上结果表明,具有识别分子DNA和拉曼信号分子DTNB的SERS纳米探针已成功制备。

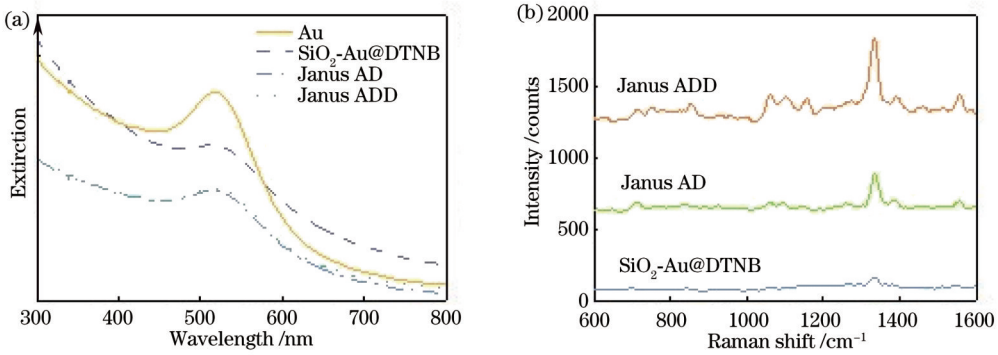

图3　SERS探针的光学特性。(a)Au、SiO_2-Au@DTNB、Janus AD和Janus ADD的消光光谱;(b)SiO_2-Au@DTNB、Janus AD和Janus ADD的SERS光谱

Fig. 3　Optical properties of SERS probes. (a) Extinction spectra of Au, SiO_2-Au@DTNB, Janus AD, and Janus ADD; (b) SERS spectra of SiO_2-Au@DTNB, Janus AD, and Janus ADD

3.2　SD水凝胶的表征

SD水凝胶通过自由基聚合反应制备。由图1(b)可知,丙烯酸酯修饰的DNA适体不仅可以连接Janus ADD,还参与SD水凝胶合成。具体而言,丙烯酸酯修饰的DNA适体(P1和P2)与Janus ADD结合,形成DNA桥。在引发剂作用下,丙烯酸酯与丙烯酰胺和双丙烯酰胺聚合,形成SD水凝胶。由于Ag胶体包含在丙烯酰胺与双丙烯酰胺组成的凝胶溶液中,因此其存在于SD水凝胶。冻干处理后,通过SEM检测SD水凝胶的结构。SEM图像清楚地显示了水凝胶的多孔结构[图4(a)]。除此之外,有无Janus ADD掺杂的水凝胶照片分别如图4(c)、(b)所示。与纯水凝胶相比,SD水凝胶呈深红色,这与Janus ADD溶液颜色一致,表明Janus ADD存在于水凝胶。以上结果表明,具有3D孔径结构的SD水凝胶已成功制备。

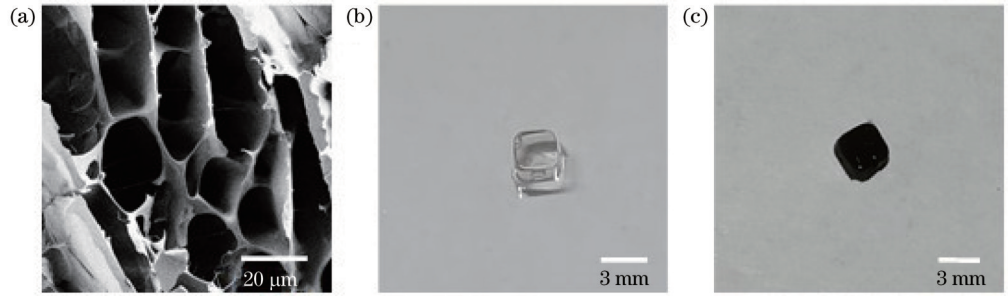

图 4　SD 水凝胶的特性。(a)SD 水凝胶的 SEM 图像;(b)纯水凝胶和(c)SD 水凝胶的照片

Fig. 4　Characteristics of SD hydrogels. (a) SEM image of SD hydrogels; photographs of (b) pure hydrogels and (c) SD hydrogels

随后,评估 SD 水凝胶的 SERS 活性。首先,研究 Ag 胶体对 SD 水凝胶中 SERS 信号影响,结果如图 5(a)所示。与不含 Ag 胶体的水凝胶相比,含 Ag 胶体的 SD 水凝胶中可以检测到更强的拉曼信号,这表明 Ag 胶体可以放大 SD 水凝胶中 SERS 探针的信号。然后,评估了 SD 水凝胶作为 SERS 基底的均匀性。在 3 个 480 μm×480 μm 的区域内,以 24 μm 的步长测量了 1323 个点的 SERS 信号,结果如图 5(b)所示。显然,不同点的 SERS 信号是均匀的,变化系数为 6%。最后,测量了 3 个批次 SD 水凝胶的 SERS 信号,其相对标准偏差(RSD)值低至 4%[图 5(c)],这对 SERS 传感器至关重要,表明 SD 水凝胶可进一步用于光学检测。

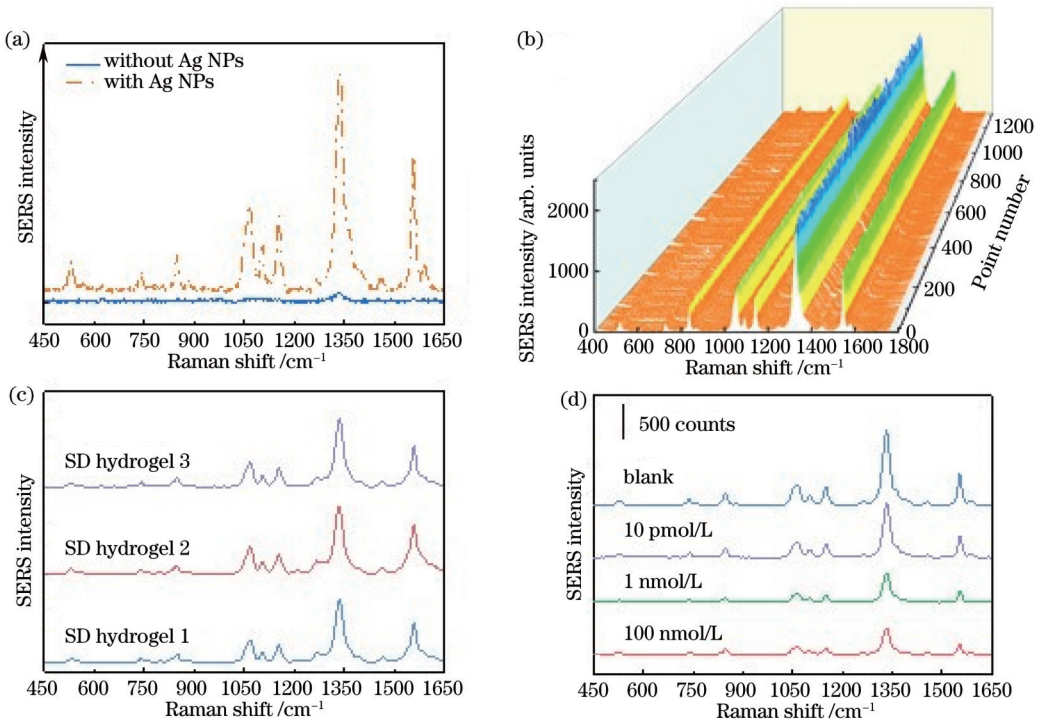

图 5　SD 水凝胶性能。(a)具有或不具有 Ag NPs 的 SD 水凝胶的 SERS 光谱;(b)从 SD 水凝胶上 3 个 480 μm×480 μm 的区域收集的 1323 个点的 SERS 光谱(背景噪声已被去除);(c)从 3 批 SD 水凝胶中收集的 SERS 光谱,对于每个 SD 水凝胶,测量 32 个点的 SERS 光谱;(d)用于检测 10 pmol/L～100 nmol/L 范围内的目标 DNA 浓度依赖性 SERS 光谱和空白对照

Fig. 5　Performance of SD hydrogels. (a) SERS spectra of SD hydrogels with or without Ag NPs; (b) SERS spectra of 1323 points collected from three areas of 480 μm×480 μm on SD hydrogels (the background noise has been removed); (c) SERS spectra collected from three batches of SD hydrogels, for each SD hydrogel, SERS spectra of 32 points were measured; (d) concentration-dependent SERS spectra for the detection of targeted DNA ranging from 10 pmol/L to 100 nmol/L and a blank control

CD63 是四通道跨膜蛋白家族成员之一,广泛存在于外泌体表面。人表皮生长因子受体 2(HER2)是肿瘤源性外泌体(包括 SKBR3 外泌体)中重要且广泛检测的特异性生物标志物。因此,选择 CD63-HER2(CH)作为适体模型,通过实验部分所述方法制备 Janus ADCH 和 SCH 水凝胶,以测试 SERS 活性 DNA 水凝胶的生物检测能力。利用 0～100 nmol/L 浓度的 CD63-HER2 互补(CHC)适体作为待测物,与 SCH 水凝胶孵育 24 h。清洗 SCH 水凝胶后,测试 SCH 水凝胶中 DTNB 的 SERS 信号强度,结果如图 5(d)所示。

由于Janus ADCH与CHC反应后脱离SCH水凝胶，因此SERS信号强度随CHC适体浓度增加而明显降低。这一结果表明，所提出的SERS活性DNA水凝胶适用于生物检测。

3.3 肿瘤源性外泌体检测

肿瘤源性外泌体携带母体癌细胞的特殊生物标志物，能够诊断早期癌症。以SKBR3外泌体为检测模型，分别通过NTA和TEM表征外泌体的尺寸和结构。NTA结果表明，SKBR3外泌体的粒径在50～200 nm范围内[图6(a)]。磷钨酸染色后，TEM图像中清楚地显示了SKBR3外泌体的囊泡结构[图6(a)插图]。NTA和TEM的检测结果证明SKBR3外泌体提取成功。

通过超分辨成像结果分析SKBR3外泌体能否进入SD水凝胶。首先，利用DID对SKBR3外泌体进行染色，并与水凝胶孵育24 h。然后，使用642 nm激光激发DID染料，以观察SKBR3外泌体的存在情况，结果如图6(b)所示。明显的荧光信号表明SKBR3外泌体存在于SD水凝胶。图6(b)的插图显示了DID标志的单个SKBR3外泌体的宽场图像(wide field)和单分子定位图像(SMLM)的合并图像。沿着实线的横截面轮廓分布表明，SMLM图像呈现约91 nm的半峰全宽，与外泌体的一般直径相等[图6(b)]。超分辨成像结果证明，外泌体可以进入SD水凝胶。

最后，将浓度为22、220、2200、22000 μL^{-1}的SKBR3外泌体分别与SERS活性DNA水凝胶孵育。将纯PBS溶液作为空白对照，所得SERS光谱如图6(c)所示。可以看到，存在目标外泌体的实验组中，SERS强度均弱于空白对照组。此外，随着外泌体浓度增加，SERS强度减弱。SKBR3外泌体浓度依赖的SERS强度生动地呈现于图6(d)。使用方程$y=169.8+221.5x$($R^2=0.987$)拟合22～22000 μL^{-1}的外泌体浓度对数与DTNB在1333 cm^{-1}处的SERS强度之间的相关性，其中y表示SERS强度，x表示外泌体浓度的对数。由此可知，所提方法可以检测浓度低至约22 μL^{-1}的外泌体。高灵敏度的检测结果表明，SERS活性DNA水凝胶在肿瘤源性外泌体检测领域具有巨大的应用潜力。

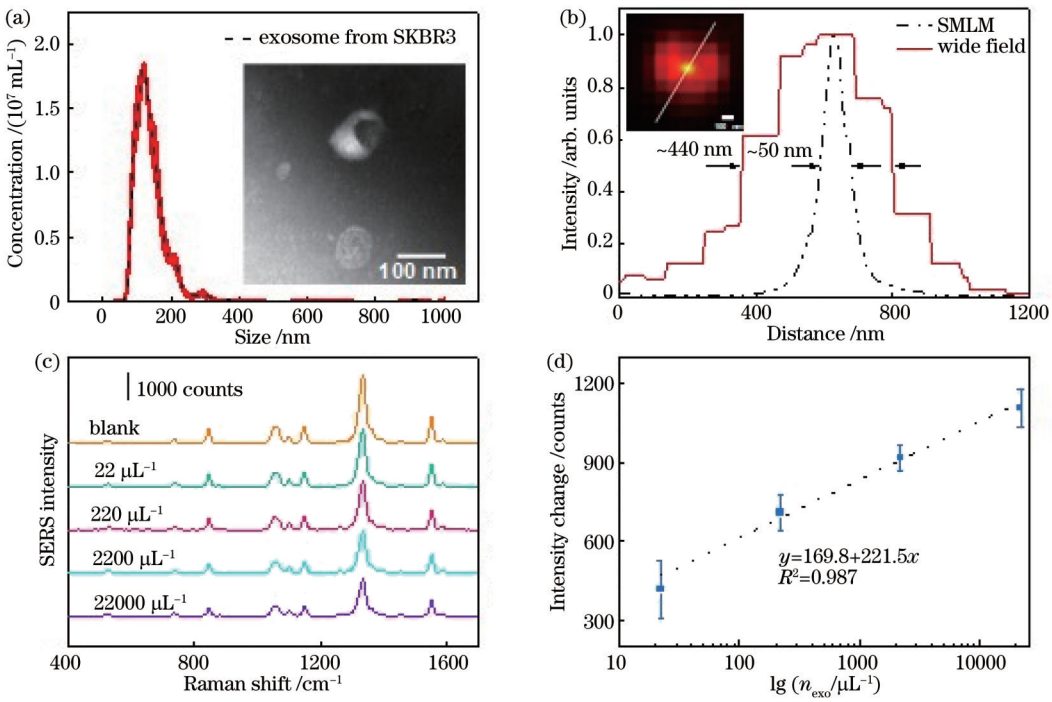

图6 外泌体检测结果。(a)SKBR3外泌体NTA实验的平均浓度随尺寸的变化(插图：SKBR3外泌体的TEM图像)；(b)DID标记的SD水凝胶中外泌体沿实线的强度分布(插图：SD水凝胶中SKBR3外泌体的超分辨图像)；(c)用于检测22～22000 μL^{-1}的SKBR3外泌体的浓度依赖性SERS光谱和空白对照；(d)目标外泌体浓度(n_{exo})依赖性信号变化，其中误差条表示8个单独测量的标准偏差，虚线是浓度相关信号变化的线性拟合

Fig. 6 Detection results of exosomes. (a) Averaged concentration versus size for NTA experiments of SKBR3 exosomes (inset: TEM image of SKBR3 exosomes); (b) intensity profiles of exosomes in SD hydrogels labeled with DID along the solid line (inset: super-resolution images of SKBR3-derived exosomes in SD hydrogels); (c) concentration-dependent SERS spectra for the detection of SKBR3-derived exosomes ranging from 22 to 22000 μL^{-1} and a blank control; (d) concentration-dependent signal change for target exosomes, the error bars represent the standard deviation for 8 individual measurements, and the dotted line is linear fitting of concentration-dependent signal change

4 结 论

通过将尺寸约3.5 nm的SERS纳米探针固定于DNA功能化聚丙烯酰胺水凝胶中，构建了一种用于肿瘤源性外泌体光学检测的功能化水凝胶（SD水凝胶）。所得SD水凝胶作为SERS活性基底具有较好的均匀性，选择1323个点测得拉曼信号分子DTNB的SERS信号变化系数约为6%；在3个批次SD水凝胶中，DTNB SERS信号的相对标准偏差约为4%。基于SERS纳米探针的识别能力和SERS信号强度变化，利用SD水凝胶实现了SKBR3外泌体的定量检测，其检测限为22 μL^{-1}，比传统的外泌体检测方法低两个数量级。所有数据表明，开发的SERS活性DNA功能化水凝胶具有优异的肿瘤源性外泌体检测性能，为癌症早期诊断提供了机会，具有广阔的应用前景。

参 考 文 献

[1] Liu C, Zhao J X, Tian F, et al. Low-cost thermophoretic profiling of extracellular-vesicle surface proteins for the early detection and classification of cancers[J]. Nature Biomedical Engineering, 2019, 3(3): 183-193.

[2] Qu M K, Lin Q, Huang L Y, et al. Dopamine-loaded blood exosomes targeted to brain for better treatment of Parkinson′s disease[J]. Journal of Controlled Release, 2018, 287: 156-166.

[3] Jeppesen D K, Fenix A M, Franklin J L, et al. Reassessment of exosome composition[J]. Cell, 2019, 177(2): 428-445.

[4] Raposo G, Stoorvogel W. Extracellular vesicles: exosomes, microvesicles, and friends[J]. The Journal of Cell Biology, 2013, 200(4): 373-383.

[5] Yáñez-Mó M, Siljander P R M, Andreu Z, et al. Biological properties of extracellular vesicles and their physiological functions[J]. Journal of Extracellular Vesicles, 2015, 4(1): 27066.

[6] Zhang X, Yuan X, Shi H, et al. Exosomes in cancer: small particle, big player[J]. Journal of Hematology & Oncology, 2015, 8: 83.

[7] Azmi A S, Bao B, Sarkar F H. Exosomes in cancer development, metastasis, and drug resistance: a comprehensive review[J]. Cancer and Metastasis Reviews, 2013, 32(3): 623-642.

[8] Zong S F, Wang L, Chen C, et al. Facile detection of tumor-derived exosomes using magnetic nanobeads and SERS nanoprobes[J]. Analytical Methods, 2016, 8(25): 5001-5008.

[9] Milane L, Singh A, Mattheolabakis G, et al. Exosome mediated communication within the tumor microenvironment[J]. Journal of Controlled Release, 2015, 219: 278-294.

[10] Melo S A, Luecke L B, Kahlert C, et al. Glypican-1 identifies cancer exosomes and detects early pancreatic cancer[J]. Nature, 2015, 523(7559): 177-182.

[11] Wei J X, Zhu K, Chen Z W, et al. Triple-color fluorescence co-localization of PD-L1-overexpressing cancer exosomes[J]. Microchimica Acta, 2022, 189(5): 182.

[12] van der Meel R, Krawczyk-Durka M, van Solinge W W, et al. Toward routine detection of extracellular vesicles in clinical samples[J]. International Journal of Laboratory Hematology, 2014, 36(3): 244-253.

[13] Zong S F, Liu Y, Yang K, et al. Eliminating nonspecific binding sites for highly reliable immunoassay via super-resolution multicolor fluorescence colocalization[J]. Nanoscale, 2021, 13(13): 6624-6634.

[14] Tavakkoli Yaraki M, Tukova A, Wang Y L. Emerging SERS biosensors for the analysis of cells and extracellular vesicles[J]. Nanoscale, 2022, 14(41): 15242-15268.

[15] 邱训, 伏秋月, 王鹏, 等. 基于表面增强拉曼光谱的致病菌检测方法研究进展[J]. 激光与光电子学进展, 2022, 59(18): 1800002.
Qiu X, Fu Q Y, Wang P, et al. Research progress on detection methods of pathogenic bacteria based on surface enhanced Raman spectroscopy[J]. Laser & Optoelectronics Progress, 2022, 59(18): 1800002.

[16] Zrimsek A B, Chiang N H, Mattei M, et al. Single-molecule chemistry with surface- and tip-enhanced Raman spectroscopy [J]. Chemical Reviews, 2017, 117(11): 7583-7613.

[17] 赖春红, 赖林, 张芝峻, 等. 基于金纳米颗粒-半胱胺SERS基底的水中硝酸根检测[J]. 中国激光, 2022, 49(11): 1111002.
Lai C H, Lai L, Zhang Z J, et al. Detection of nitrate in water based on gold nanoparticles-cysteamine SERS substrate[J]. Chinese Journal of Lasers, 2022, 49(11): 1111002.

[18] Wang Z Y, Zong S F, Wu L, et al. SERS-activated platforms for immunoassay: probes, encoding methods, and applications [J]. Chemical Reviews, 2017, 117(12): 7910-7963.

[19] Zong C, Xu M X, Xu L J, et al. Surface-enhanced Raman spectroscopy for bioanalysis: reliability and challenges[J]. Chemical Reviews, 2018, 118(10): 4946-4980.

[20] Wu L, Teixeira A, Garrido-Maestu A, et al. Profiling DNA mutation patterns by SERS fingerprinting for supervised cancer classification[J]. Biosensors and Bioelectronics, 2020, 165: 112392.

[21] Yang K, Zhu K, Wang Y Z, et al. $Ti_3C_2T_x$ MXene-loaded 3D substrate toward on-chip multi-gas sensing with surface-enhanced Raman spectroscopy (SERS) barcode readout[J]. ACS Nano, 2021, 15(8): 12996-13006.

[22] 刘磊, 卞正兰, 董作人, 等. 山药中有机农药残留的表面增强拉曼光谱检测[J]. 激光与光电子学进展, 2022, 59(4): 0417001.
Liu L, Bian Z L, Dong Z R, et al. Detection of residual organic pesticides in yam by surface enhanced Raman spectroscopy[J]. Laser & Optoelectronics Progress, 2022, 59(4): 0417001.

[23] Liu Z R, Li T Y, Wang Z Y, et al. Gold nanopyramid arrays for non-invasive surface-enhanced Raman spectroscopy-based gastric cancer detection via sEVs[J]. ACS Applied Nano Materials, 2022, 5(9): 12506-12517.

[24] Wang J, Xie H Y, Ding C F. Designed co-DNA-locker and ratiometric SERS sensing for accurate detection of exosomes based on gold nanorod arrays[J]. ACS Applied Materials & Interfaces, 2021, 13(28): 32837-32844.

[25] Zhu K, Wang Z Y, Zong S F, et al. Hydrophobic plasmonic nanoacorn array for a label-free and uniform SERS-based biomolecular assay[J]. ACS Applied Materials & Interfaces, 2020, 12(26): 29917-29927.

[26] Hou M, He D G, Bu H C, et al. A sandwich-type surface-enhanced Raman scattering sensor using dual aptamers and gold nanoparticles for the detection of tumor extracellular vesicles[J]. The Analyst, 2020, 145(19): 6232-6236.

[27] Wang Z L, Zong S F, Wang Y J, et al. Screening and multiple detection of cancer exosomes using an SERS-based method[J]. Nanoscale, 2018, 10(19): 9053-9062.

[28] Pan H M, Dong Y, Gong L B, et al. Sensing gastric cancer exosomes with MoS_2-based SERS aptasensor[J]. Biosensors and Bioelectronics, 2022, 215: 114553.

[29] Shao R Y, Wang Y B, Li L F, et al. Bone tumors effective therapy through functionalized hydrogels: current developments and future expectations[J]. Drug Delivery, 2022, 29(1): 1631-1647.

[30] Jiang S H, Deng J J, Jin Y H, et al. Breathable, antifreezing, mechanically skin-like hydrogel textile wound dressings with dual antibacterial mechanisms[J]. Bioactive Materials, 2023, 21: 313-323.

[31] Dave N, Chan M Y, Huang P J J, et al. Regenerable DNA-functionalized hydrogels for ultrasensitive, instrument-free mercury (Ⅱ) detection and removal in water[J]. Journal of the American Chemical Society, 2010, 132(36): 12668-12673.
[32] Li Z T, Cheng E J, Huang W X, et al. Improving the yield of mono-DNA-functionalized gold nanoparticles through dual steric hindrance[J]. Journal of the American Chemical Society, 2011, 133(39): 15284-15287.
[33] Pham T, Jackson J B, Halas N J, et al. Preparation and characterization of gold nanoshells coated with self-assembled monolayers[J]. Langmuir, 2002, 18(12): 4915-4920.
[34] Lee P C, Meisel D. Adsorption and surface-enhanced Raman of dyes on silver and gold sols[J]. The Journal of Physical Chemistry, 1982, 86(17): 3391-3395.

Functionalized Hydrogel for Highly Sensitive Detection of Tumor-Derived Exosomes

Yang Zhaoyan[1,2], Zhao Shujin[1], Wang Ziye[1], Liu Jiao[1], Zong Shenfei[2], Wang Zhuyuan[2**], Li Bingxiang[1*], Cui Yiping[2]

[1]*College of Electronic and Optical Engineering & College of Flexible Electronics (Future Technology), Nanjing University of Posts and Telecommunications, Nanjing* 210023, *Jiangsu, China*;
[2]*School of Electronic Science and Engineering, Southeast University, Nanjing* 210096, *Jiangsu, China*

Abstract

Objective Exosomes play a vital role in intracellular communications and the exchange of substances. Compared with normal cells, tumor cells secrete more exosomes with tumor-specific proteins, which makes tumor-derived exosomes an important kind of cancer biomarker. Thus, the detection of tumor-derived exosomes can provide critical information for the diagnosis of cancer. However, the current detection methods for tumor-derived exosomes still have some shortcomings, including tedious operation and limited accuracy. It is necessary to develop a method with convenient operation and high sensitivity to detect exosomes. Surface-enhanced Raman spectroscopy (SERS) has been widely applied in the biological detection fields due to its excellent optical properties. SERS-based exosome detection methods have flourished in recent years. Many materials have been combined with SERS probes to achieve optimal detection results. Hydrogels are water-swellable polymeric materials with a three-dimensional (3D) network structure synthesized by crosslinking hydrophilic polymers. The porous structure of hydrogels is similar to that of the extracellular matrix. Specifically, acrydite-modified DNA can be easily incorporated into hydrogels during gel formation to recognize and immobilize biomolecules. More importantly, biomolecules can retain their intrinsic structure and function in hydrogels. Therefore, we wish to realize highly efficient and sensitive detection of tumor-derived exosomes by combining the SERS probe with hydrogels.

Methods We demonstrate an optical detection of tumor-derived exosomes by developing SERS-active DNA functionalized hydrogels (denoted as SD hydrogels). The details of detection are presented in Fig. 1. SD hydrogels consist of two parts. One is SERS nanoprobes for the recognition of exosomes and the generation of SERS signals [Fig. 1(a)], and the other is DNA-functionalized polyacrylamide hydrogels (denoted as DPAAm hydrogels) for the immobilization of SERS nanoprobes and the amplification of Raman signals. These two parts are connected by the DNA in DPAAm hydrogels [Fig. 1(b)]. Figure 1(c) presents the detection principle of SD hydrogels for tumor-derived exosomes. Generally, SERS nanoprobes contain two recognition units, or in other words, one applies to all exosomes, and the other is only suitable for tumor-derived exosomes. Such an SD hydrogel takes advantage of SERS nanoprobes to distinguish the difference in the surface specific proteins between tumor and normal cells derived exosomes. Once tumor-derived exosomes appear, the interaction between SERS nanoprobes and DNA in DPAAm hydrogels is broken, followed by SERS nanoprobes falling from hydrogels with the help of PBS buffer, resulting in the weak SERS signals on account of the concentration of tumor-derived exosomes.

Results and Discussions To obtain SERS probes (denoted as Janus ADD), Au NPs with about 3.5 nm diameter are modified by Raman reporter (DTNB) and recognition unit as DNA. The experimental results display that Janus ADD possesses a well-distinguishable Raman signal and has been functionalized with DNA (Figs. 2 and 3). Then, Janus ADD is immobilized into SD hydrogels by the acrydite-modified DNA aptamers. SEM image clearly demonstrates the porous structure of hydrogel [Fig. 4(a)]. The photographs indicate that SD hydrogels containing Janus ADD have been fabricated successfully. Subsequently, the features of SD hydrogels as SERS-active substrates are evaluated. The results show that SD hydrogels have the ability to amplify the Raman signals of Janus ADD, and the SERS signals at different points of SD

hydrogels are homogeneous with a coefficient of variation of 6%. Besides, the SERS signals of three individual SD hydrogels have a relative standard deviation (RSD) value as low as 4%, which is of key importance for SERS sensors. Further, the detection ability of SD hydrogels is proved by the complementary aptamers at different concentrations ranging from 0 to 100 nmol/L in PBS solution. The SERS intensity of DTNB in SD hydrogels distinctly decreases with the increased concentration of complementary aptamers, indicating that SD hydrogels are suitable for biological detection. Finally, SD hydrogels are used to detect tumor-derived exosomes. SKBR3 exosomes are selected as a model and isolated from the cell media of SKBR3 cell lines. The obtained SKBR3 exosomes are consistent with the previous reports in vesicle structure and particle size. Moreover, SKBR3 exosomes can be observed in SD hydrogels by a super-resolution microscope. The concentration-dependent SERS intensity indicates that the SERS intensity decreases as the number of exosomes increases, and the SERS signals in target exosome groups are obviously much weaker than that of the blank control (Fig. 6). As a result, the limit of detection (LOD) of the present method is found to be approximately 22 μL^{-1}. The high sensitivity evidences that the SD hydrogels possess huge potential for the detection of tumor-derived exosomes in an easy and inexpensive manner at the point of care.

Conclusions In this paper, SD hydrogels have been established to optically detect SKBR3-derived exosomes by immobilizing SERS nanoprobes into DNA-functionalized hydrogels. The SERS nanoprobes are used to recognize SKBR3-derived exosomes and generate fingerprint signals. DNA functionalized hydrogels serve a variety of functions, including providing a biocompatible environment for exosomes, supplying abundant sites for immune reaction, and amplifying Raman signals of SERS probes. The obtained SD hydrogel as a SERS active substrate has high uniformity, and the SERS signals obtained from DTNB by measuring at 1323 points have a coefficient of variation of 6%. Besides, the relative standard deviation of the SERS signal about DTNB in the three batches of SD hydrogels is about 4%. By taking advantage of the specific recognition ability and excellent Raman enhancement effect, the SD hydrogels are applied to the quantitative detection of SKBR3 exosomes with an ultralow LOD of about 22 μL^{-1}, which is two orders of magnitude lower than that of the conventional exosome detection methods. In view of the diversity of SERS probes, such an SD hydrogel is promising as a universal sensor for the detection of tumor-derived exosomes.

Key words bio-optics; surface-enhanced Raman scattering spectroscopy; optical detection; exosome; nanoprobe; hydrogel